Structural Engineering and Mechanics, Vol. 30, No. 3 (2008) 317-330
DOI: http://dx.doi.org/10.12989/sem.2008.30.3.317

Variations of the stress intensity factors for a planar crack parallel to a bimaterial interface

Chunhui Xu†, Taiyan Qin‡ and Li Yuan‡†

College of Science, China Agricultural University, Beijing 100083, P.R. China

Nao-Aki Noda‡‡

Department of Mechanical Engineering, Kyushu Institute of Technology, Kitakyushu, 804-8550, Japan

(Received April 7, 2007, Accepted August 19, 2008)

Abstract. Stress intensity factors for a planar crack parallel to a bimaterial interface are considered. The formulation leads to a system of hypersingular integral equations whose unknowns are three modes of crack opening displacements. In the numerical analysis, the unknown displacement discontinuities are approximated by the products of the fundamental density functions and polynomials. The numerical results show that the present method yields smooth variations of stress intensity factors along the crack front accurately. The mixed mode stress intensity factors are indicated in tables and figures with varying the shape of crack, distance from the interface, and elastic constants. It is found that the maximum stress intensity factors normalized by root area are always insensitive to the crack aspect ratio. They are given in a form of formula useful for engineering applications.

Keywords: hypersingular integral equation; stress intensity factor; bimaterial; crack.

1. Introduction

In recent years, composite materials and adhesive or bonded joints are being used in wide range of engineering field. Although a lot of researches have been made in terms of fracture mechanics approach regarding interface, most of them generally involve two dimensional modeling (Erdogan and Aksogan 1974, Cook and Erdogan 1972, Isida and Nogushi 1983, Afsar and Ahmed 2005, Itou 2007, Qiao and Wang 2004, Chen *et al*. 2003, Kao-Walter *et al*. 2006, Kaddouri *et al*. 2006, Huang and Kardomateas 2001, Chang and Xu 2007, Takeda *et al*. 2004). Few works have been carried out for the three dimensional crack problems except those of specially shaped cracks (Willis 1972, Kassir and Bregman 1972, Shibuya *et al*. 1989, Lee *et al.* 1987). This is mainly due to the extreme difficulties of solving such problems by mathematics and mechanics, or to the substantial computation required in the numerical analyses. Itou (2007) investigated the stress intensity factors

† Associate Professor, E-mail: xuchunhui-cau@163.com
‡ Professor, Corresponding author, E-mail: tyqin@cau.edu.cn
‡† Master Student, E-mail: katsu-000@163.com
‡‡ Professor, E-mail: noda@mech.kyutech.ac.jp

for an interface crack between an epoxy and aluminum composite plate under a tensile load. Qiao and Wang (2004) presented an elastic deformable crack tip model which can improve the split beam solution, and obtained explicit closed-form solutions for ERR and SIF for which both the transverse shear and crack tip deformation effects are accounted. Kao-Walter *et al*. (2006) investigated the crack tip driving force of a crack growing from a pre-crack that is perpendicular to and terminating at an interface between two materials by the finite element method. Kaddouri *et al.* (2006) analyzed the interaction effect between a crack and an interface in a ceramic/metal bi-material and discussed the effects of the elastic properties of two bonded materials, the distance between the crack tip and the interface. Huang (2001) presented a method for obtaining the mixed-mode stress intensity factors for bimaterial interface cracks or cracks parallel to the bimaterial interface in half-plane configurations. Chang and Xu (2007) proposed a pair of contour integrals $J_{k\varepsilon}$, and presented the relationship between $J_{k\varepsilon}$ and the generalized stress intensity factors. Takeda *et al.* (2004) investigated the stress intensity factors for several crack configurations in G-11 woven glass/epoxy laminates under tension at cryogenic temperatures by the finite element method, and obtained the order of stress singularities at the tip of a crack. In the previous study (Chen *et al.* 1999), the integral equations for the crack parallel to a bimaterial interface were formulated as a system of singular equation. Then Noda *et al*. (2003) dealt with an elliptical crack parallel to an interface on the basis of the above equations. Qin *et al.* ((2002, 2003) analyzed a planar crack terminating at an interface using a hypersingular integral equation method, and given the mode I numerical solutions of the stress intensity factors of a rectangular crack. In this study, the numerical method is proposed for a rectangular crack parallel to an interface. The equations will be solved accurately by using fundamental densities and polynomials to approximate unknown functions, where the fundamental densities are chosen to express the stress fields due to the rectangular crack in an infinite body exactly. Then the stress intensity factors will be indicated with varying shape of the crack, elastic constants of materials, and the distance between the crack and interface.

2. Hypersingular integral equations for a planar crack parallel to a bimaterial interface

Consider a planar crack parallel to a bimaterial interface, under tension σ_z^∞ at infinity as shown in Fig. 1. Two dissimilar elastic half-spaces bonded together along the $x-y$ plane, (see Fig. 1) with a fixed rectangular Cartesian coordinate system *x*, *y*, *z*.

Suppose that the upper half-space is occupied by an elastic medium with constants (μ_1, ν_1) and the lower half-space by an elastic medium with constants (μ_2, ν_2), here μ_1, μ_2 are the shear modulus, and ν_1, ν_2 are the Poisson's ratio. The planar crack is assumed to be located at a distance *h* above, and parallel to the bimaterial interface. The displacements in the upper space I due to the crack disturbance can be expressed in terms of Somigliana's identity as

$$u_i(x,y,z) = -\iint_{S^+} \overset{+}{T}_{ij}(x,y,z,\xi,\eta)\Delta u_j(\xi,\eta)d\xi d\eta \qquad i,j = x,y,z \tag{1}$$

In which $\Delta u_j(\xi,\eta) = u_j^+(\xi,\eta) - u_j^-(\xi,\eta)$ is the unknown displacement discontinuity across the crack surfaces $(S^\pm)$, $\overset{+}{T}_{ij}(x,y,\xi,\eta)$ denotes the tractions in the *j*-direction at a point (ξ,η,h) of the upper crack surface generated by a unit concentrated body force in the *i*-direction applied at a point (x,y,z) in the half space.

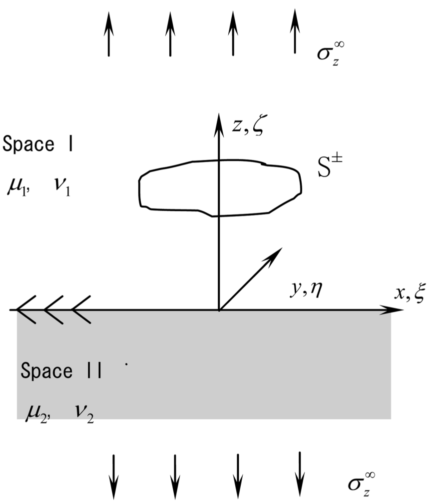

Fig. 1 A planar crack parallel to a bimaterial interface

The corresponding stress field is given as follow

$$\sigma_{ij}(x,y,z) = \iint_S \left\{ \frac{2\mu_1 \nu_1}{1-2\nu_1} \frac{\partial T_{kl}(x,y,z,\xi,\eta)}{\partial x_k} \delta_{ij} + \mu_1 \left[\frac{\partial T_{il}(x,y,z,\xi,\eta)}{\partial x_j} + \frac{\partial T_{jl}(x,y,z,\xi,\eta)}{\partial x_i} \right] \right\} \Delta u_l(\xi,\eta) ds(\xi,\eta) \tag{2}$$

Using the boundary condition, the hypersingular integral equation for unknown function can be obtained.

$$\frac{\mu_1}{4\pi(1+\kappa_1)} \left\{ \oint\!\!\!\oint_s \frac{1}{r^3} [2(\kappa_1 - 1)\delta_{\alpha\beta} + 3(3-\kappa_1) r_{,\alpha} r_{,\beta}] \Delta u_\beta(\xi,\eta) \mathrm{d}\xi \mathrm{d}\eta \right.$$

$$\left. + \iint_s K_{\alpha i}(\xi,\eta,x,y) \Delta u_i(\xi,\eta) \mathrm{d}\xi \mathrm{d}\eta \right\} = -p_\alpha(x,y) \qquad \alpha = x,y \tag{3a}$$

$$\frac{\mu_1}{4\pi(1+\kappa_1)} \oint\!\!\!\oint_s \left[\frac{4}{r^3} \delta_{zi} + K_{zi}(\xi,\eta,x,y) \right] \Delta u_i(\xi,\eta) \mathrm{d}\xi \mathrm{d}\eta = -p_z(x,y) \tag{3b}$$

where

$$K_{xx} = -[(\kappa_1 - 1) + (\kappa_1 + 1)(\Lambda_1 + \Lambda_2 - 2\Lambda)] \frac{2}{R^3} + 3\{4(\kappa_1 - 5) + 2(\kappa_1 + 1)(3\Lambda_1 - \Lambda_2)]h^2 - [(3-\kappa_1)$$

$$+ 2(\kappa_1 + 1)(\Lambda - \Lambda_1 - \Lambda_2)](x-\xi)^2\} \frac{1}{R^5} + 120[1 - (\kappa_1 + 1)\Lambda_1] h^2 [4h^2 + 3(x-\xi)^2] \frac{1}{R^7} \tag{4a}$$

$$-3360[1 - (\kappa_1 + 1)\Lambda_1] h^4 (x-\xi)^2 \frac{1}{R^9}$$

$$K_{yx} = -3(x-\xi)(y-\eta) \left\{ [(3-\kappa_1) + 2(\kappa_1 + 1)(\Lambda - \Lambda_1 - \Lambda_2)] \frac{1}{R^5} - 40[1 - (\kappa_1 + 1)\Lambda_1] \left(\frac{3h^2}{R^7} - \frac{28h^4}{R^9} \right) \right\} \tag{4b}$$

$$K_{zx} = -12h(x-\xi)\left\{(\kappa_1+1)(\Lambda_1-\Lambda_2)\frac{1}{R^5} - 20[1-(\kappa_1+1)\Lambda_1]\left(\frac{3h^2}{R^7} - \frac{28h^4}{R^9}\right)\right\} \tag{4c}$$

$$K_{zz} = -[2-(\kappa_1+1)(\Lambda_1+\Lambda_2)]\frac{2}{R^3} + 24h^2\left\{[(\kappa_1+1)(\Lambda_1-\Lambda_2)-1]\frac{1}{R^5} - 80[1-(\kappa_1+1)\Lambda_1]h^2\left(\frac{1}{R^7} - \frac{7h^2}{R^9}\right)\right\} \tag{4d}$$

$$K_{yy}(x, y, \xi, \eta) = K_{xx}(x \to y, \xi \to \eta) \tag{4e}$$

$$K_{xy}(x, y, \xi, \eta) = K_{yx}(x, y, \xi, \eta) \tag{4f}$$

$$K_{zy}(x, y, \xi, \eta) = K_{zx}(x \to y, \xi \to \eta) \tag{4g}$$

$$K_{xz}(x, y, \xi, \eta) = -K_{zx}(x, y, \xi, \eta) \tag{4h}$$

$$K_{yz}(x, y, \xi, \eta) = -K_{zy}(x, y, \xi, \eta) \tag{4i}$$

$$\Lambda = \frac{\mu_2}{\mu_1+\mu_2},\ \Lambda_1 = \frac{\mu_2}{\mu_1+\kappa_1\mu_2},\ \Lambda_2 = \frac{\mu_2}{\mu_2+\kappa_2\mu_1},\ \kappa_1 = 3-4\nu_1,\ \kappa_2 = 3-4\nu_2$$

$$r^2 = (x-\xi)^2 + (y-\eta)^2,\ R^2 = r^2 + 4h^2 \tag{4j}$$

Eqs. (3a)-(3b) enforce boundary conditions at the prospective boundary S for crack. Here, (p_x, p_y, p_z) represent the loadings on the crack surface due to internal or external loadings, which can been obtained from the solution for the loadings of the uncracked solid. The integration $\oint\!\!\oint_s$ should be interpreted in a sense of a finite part integral in the region S.

3. Numerical methods of singular integral equations

Consider a rectangular crack parallel to a bimaterial interface, under tension σ_z^∞ at infinity. Here the dimensions of rectangular crack are $2a\times 2b$. In the numerical solution, it is necessary to express the singular stresses, which are specific at the crack tip. In the present analysis, the fundamental density functions are chosen to express the stress field due to a single interface crack exactly and the following expressions have been used to approximate the unknown functions.

$$\Delta u_i(\xi, \eta) = F_i(\xi, \eta)\sqrt{a^2-\xi^2}\sqrt{b^2-\eta^2} \tag{5}$$

Here, the following expressions can be applied, where the unknowns are coefficients of the polynomials:

$$F_i(\xi, \eta) = a_{i0} + a_{i1}\eta + \ldots + a_{i(n-1)}\eta^{(n-1)} + a_{in}\eta^n + a_{i(n+1)}\xi + a_{i(n+2)}\xi\eta + \ldots$$

$$+ a_{i(2n)}\xi\eta^n + \ldots + a_{i(N-n-1)}\xi^m + a_{i(N-n)}\xi^m\eta + \ldots + a_{i(N-1)}\xi^m\eta^n = \sum_{i=0}^{N-1} a_{il}G_l(\xi, \eta) \quad i = x, y, x$$

$$N = (m+1)(n+1)$$

$$G_0(\xi, \eta) = 1, \quad G_1(\xi, \eta) = \eta, \ldots, G_{n+1}(\xi, \eta) = \xi, \ldots, G_{N-1}(\xi, \eta) = \xi^m \eta^n$$

Using the approximation method mentioned above, we obtain the following system of algebraic equations for the determination of coefficients a_{il} ($i = x, y, z$), which can be determined by selecting a set of collocation points.

$$\left.\begin{aligned} \sum_{l=0}^{N-1} a_{\beta l} f_{\alpha\beta l}^{1} + \sum_{l=0}^{N-1} a_{il} f_{\alpha il}^{2} &= -\frac{4\pi(1+\kappa_1)}{\mu_1} p_\alpha \\ \sum_{l=0}^{N-1} a_{zl} f_{zzl}^{1} + \sum_{l=0}^{N-1} a_{il} f_{zil}^{2} &= -\frac{4\pi(1+\kappa_1)}{\mu_1} p_z \end{aligned}\right\} \quad i = x, y, z;\ \alpha, \beta = x, y \tag{6}$$

The number of unknowns in Eq. (6) is $3l$. As examples, $f_{\alpha\beta l}^{1}, f_{zzl}^{1}, f_{\alpha il}^{2}, f_{zil}^{2}$ are expressed as follows

$$f_{\alpha\beta l}^{1} = \iint_s \frac{1}{r^3}[2(\kappa_1 - 1)\delta_{\alpha\beta} + 3(3-\kappa_1) r_{,\alpha} r_{,\beta}] G_l(\xi, \eta)\sqrt{a^2-\xi^2}\sqrt{b^2-\eta^2}\,\mathrm{d}s(\xi, \eta) \tag{7a}$$

$$f_{zzl}^{1} = \iint_s \frac{4}{r^3} G_l(\xi, \eta)\sqrt{a^2-\xi^2}\sqrt{b^2-\eta^2}\,\mathrm{d}s(\xi, \eta) \tag{7b}$$

$$f_{\alpha il}^{2} = \iint_s K_{\alpha i}(\xi, \eta, x, y)\sqrt{a^2-\xi^2}\sqrt{b^2-\eta^2}\, G_l(\xi, \eta)\,\mathrm{d}s(\xi, \eta) \tag{7c}$$

$$f_{zil}^{2} = \iint_s K_{zi}(\xi, \eta, x, y)\sqrt{a^2-\xi^2}\sqrt{b^2-\eta^2}\, G_l(\xi, \eta)\,\mathrm{d}s(\xi, \eta) \tag{7d}$$

In Eqs. (7c) and (7d), the integrals can be evaluated numerically because of no singularities in the integral. However, the integrals in Eq. (7a) and Eq .(7b) have a hypersingularity of the form r^{-3} when $x = \xi$ and $y = \eta$, and it cannot be evaluated in the present form. Using the Taylor's expansion with the local polar coordinates system $\xi - x = r\cos\theta$, $\eta - y = r\sin\theta$ as shown in Fig. 2, the following expressions are given, and they will be applied to evaluate the integral.

$$\sqrt{a^2-\xi^2} = P_0(x) - (\xi - x)P_1(x) - (\xi - x)^2 P_2(\xi - x)$$

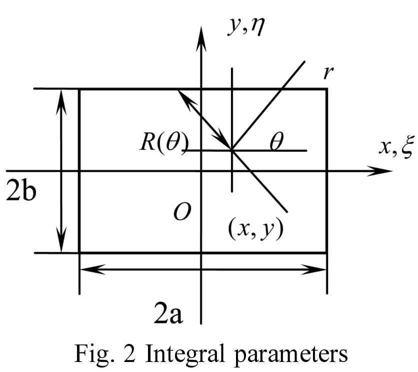

Fig. 2 Integral parameters

$$\sqrt{b^2-\eta^2} = Q_0(y)-(\eta-y)Q_1(y)-(\eta-y)^2Q_2(\eta,y)$$

$$\xi^m = x^m + mx^{m-1}(\xi-x)+\sum_{i=0}^{m-2}[(i+1)\xi^{(m-2-i)}x^i](\xi-x)^2 = b_0(x)+b_1(x)(\xi-x)+b_2(\xi,x)(\xi-x)^2$$

$$\eta^n = x^n + nx^{n-1}(\eta-y)+\sum_{i=0}^{n-2}[(i+1)\eta^{(n-2-i)}y^i](\eta-y)^2 = c_0(y)+c_1(y)(\eta-y)+c_2(\eta,y)(\eta-y)^2 \quad (8)$$

Here

$$P_0(x) = \sqrt{a^2-x^2}, \qquad P_1(x) = \frac{x}{\sqrt{a^2-x^2}}$$

$$P_2(\xi,x) = \frac{\xi+x}{\sqrt{a^2-x^2}(\sqrt{a^2-\xi^2}+\sqrt{a^2-x^2})} \times \frac{a^2}{(\xi\sqrt{a^2-x^2}+x\sqrt{a^2-\xi^2})}$$

$$Q_0(x) = \sqrt{b^2-y^2}, \qquad Q_1(x) = \frac{y}{\sqrt{b^2-y^2}}$$

$$Q_2(\eta,y) = \frac{\eta+y}{\sqrt{b^2-y^2}(\sqrt{a^2-\eta^2}+\sqrt{b^2-y^2})} \times \frac{b^2}{(\eta\sqrt{b^2-y^2}+y\sqrt{b^2-\eta^2})}$$

Using the concept of finite-part integral method and the relations (8), the hypersingular integrals in Eq. (7a) and Eq. (7b) can be reduced in the following form.

$$f^1_{\alpha\beta l}(x,y) = \int_0^{2\pi}\int_0^{R(\theta)}\left[\frac{D_0(x,y)}{r^2}+\frac{D_1(\theta)}{r}+D_2(r,\theta)\right][2(\kappa_1-1)\delta_{\alpha\beta}+3(3-\kappa_1)r_{,\alpha}r_{,\beta}]\mathrm{d}r\mathrm{d}\theta$$

$$= \int_0^{2\pi}\left[-\frac{D_0(x,y)}{R(\theta)}+D_1(x,y,\theta)\ln(R(\theta))+\int_0^{R(\theta)}D_2(x,y,r,\theta)\mathrm{d}r\right][2(\kappa_1-1)\delta_{\alpha\beta}+3(3-\kappa_1)r_{,\alpha}r_{,\beta}]\mathrm{d}\theta \quad \text{(9a)}$$

$$f^1_{zzl}(x,y) = 4\int_0^{2\pi}\int_0^{R(\theta)}\left[\frac{D_0(x,y)}{r^2}+\frac{D_1(\theta)}{r}+D_2(r,\theta)\right]\mathrm{d}r\mathrm{d}\theta$$

$$= \int_0^{2\pi}4\left[-\frac{D_0(x,y)}{R(\theta)}+D_1(x,y,\theta)\ln(R(\theta))+\int_0^{R(\theta)}D_2(x,y,r,\theta)\mathrm{d}r\right]\mathrm{d}\theta \quad \text{(9b)}$$

where $r_{,x}=\cos\theta, r_{,y}=\sin\theta$, and $D_0(x,y), D_1(x,y,\theta)$ and $D_2(x,y,r,\theta)$ are known functions, which can be expressed as a combination of Eq. (8). Now the integrals in (9) are general ones, and can be calculated numerically. The notation $R(\theta)$ means a distance between a point (x,y) in question and a point on the fictitious boundary of the crack as shown in Fig. 2.

4. Numerical results and discussion

Consider a rectangular crack parallel to bimaterial interface under a uniform tension load σ_z^∞. In demonstrating the numerical results of stress intensity factors (SIFs), the following dimensionless factors F_I, F_{II} and F_{III} will be used.

$$F_I = \frac{K_I(\xi, \eta)}{\sigma_z^\infty \sqrt{\pi b}} = \sqrt{a^2 - \xi^2} F_z(\xi, \eta)\Big|_{\eta = \pm b}$$

$$F_{II} = \frac{K_{II}(\xi, \eta)}{\sigma_z^\infty \sqrt{\pi b}} = \sqrt{a^2 - \xi^2} F_y(\xi, \eta)\Big|_{\eta = \pm b}$$

$$F_{III} = \frac{K_{III}(\xi, \eta)}{\sigma_z^\infty \sqrt{\pi b}} = (1 - \nu_1)\sqrt{a^2 - \xi^2} F_x(\xi, \eta)\Big|_{\eta = \pm b} \tag{10}$$

In the following discussion, the maximum stress intensity factors F_I and F_{II} appearing at (0, b) (or (0, $-b$)) will be mainly considered. In addition, the results using Murakami's $\sqrt{area}$ parameter will be also discussed (Murakami 1985, Murakami and Endo 1983, Murakami and Isida 1985, Murakami and Nemat-Nasser 1983, Murakami *et al.* 1988). Here "area" is the projected area of the defect or crack. For the cracks subjected to tension σ_z^∞ (Murakami 1985, Murakami and Endo 1983)

$$K_{\mathrm{Imax}} = 0.50\sigma_z^\infty \sqrt{\pi\sqrt{area}}$$

For the crack subjected to shear τ_{yz}^∞ (Murakami and Isida 1985, Murakami and Nemat-Nasser 1983, Murakami *et al.* (1988):

$$K_{\mathrm{IImax}} = 0.55\,\tau_{yz}^\infty \sqrt{\pi\sqrt{area}} \quad (a/b \geq 1)$$

$$K_{\mathrm{IIImax}} = 0.45\,\tau_{yz}^\infty \sqrt{\pi\sqrt{area}} \quad (a/b \leq 1)$$

where "*area*" is the projected area of the crack or defects. In this paper, for rectangular crack, $area = 4ab$. However, it should be noted that $area = 20b^2$ when $a/b \geq 5$, and $area = 20a^2$ when $a/b \leq 0.2$.

$$F_I^* = \frac{K_I(\xi, \eta)}{\sigma_z^\infty \sqrt{\pi\sqrt{area}}} = \left(\frac{b}{4a}\right)^{1/4} F_I$$

$$F_{II}^* = \frac{K_{II}(\xi, \eta)}{\sigma_z^\infty \sqrt{\pi\sqrt{area}}} = \left(\frac{b}{4a}\right)^{1/4} F_{II}$$

$$F_{III}^* = \frac{K_{III}(\xi, \eta)}{\sigma_z^\infty \sqrt{\pi\sqrt{area}}} = \left(\frac{b}{4a}\right)^{1/4} F_{III} \tag{11}$$

4.1 Compliance of boundary condition and convergence of numerical solutions

Figs. 3(a)-(c) show the compliance of boundary condition along the crack surface for $a/b = 1$, $\nu_1 = \nu_2 = 0.3$, $\mu_2/\mu_1 = 0$, $h/2b = 0.4$, where the collocation point number is 400(20×20), polynomial exponent are taken as $m = n = 8$. It is shown that the remaining stresses $\sigma_z/\sigma_z^\infty + 1$, $\tau_{zx}/\sigma_z^\infty$, and $\tau_{yx}/\sigma_z^\infty$ on the surface are less than 1.5×10^{-5}, when $m = n = 8$.

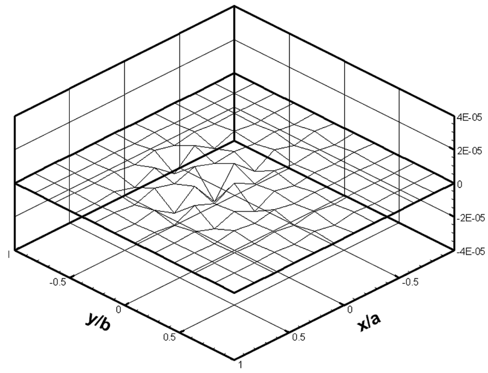

(a) $\frac{\sigma_z}{\sigma_z^\infty}+1 \cong 0$

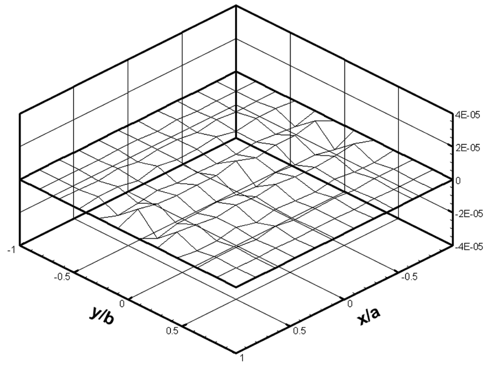

(b) $\frac{\tau_{yz}}{\sigma_z^\infty} \cong 0$

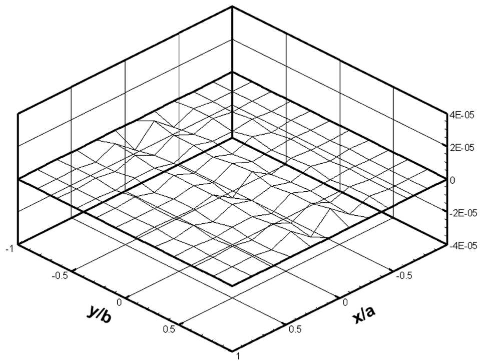

(c) $\frac{\tau_{zx}}{\sigma_z^\infty} \cong 0$

Fig. 3 Compliance of boundary condition for $\nu_1 = \nu_2 = 0.3$, $\mu_2/\mu_1 = 0$, $h/2b = 0.4$

Table 1(a) Convergence of the results F_I and F_{II} when $\mu_2/\mu_1 = 0$, $\nu_1 = \nu_2 = 0.3$

			$h/2b$					
a/b		n	0.2	0.3	0.4	0.5	1.0	2.0
1	F_I	6	1.828	1.312	1.0928	0.9765	0.8017	0.7609
		7	1.833	1.314	1.0932	0.9765	0.8017	0.7609
		8	1.850	1.315	1.0932	0.9765	0.8017	0.7609
	F_{II}	6	0.4626	0.2146	0.1175	0.0698	0.00962	0.00083
		7	0.4709	0.2212	0.1183	0.0699	0.00962	0.00083
		8	0.4716	0.2213	0.1183	0.0699	0.00962	0.00083
16	F_I	6	2.900	2.078	1.7127	1.5095	1.1629	1.0453
		7	2.923	2.083	1.7131	1.5104	1.1632	1.0453
		8	2.943	2.085	1.7131	1.5104	1.1632	1.0453
	F_{II}	6	0.9492	0.4852	0.2888	0.1848	0.0367	0.00550
		7	0.9690	0.4957	0.2893	0.1850	0.0368	0.00550
		8	0.9706	0.4958	0.2893	0.1850	0.0368	0.00550

Table 1(b) Convergence of the results F_I and F_{II} when $\mu_2/\mu_1 = 0$, $\nu_1 = \nu_2 = 0.3$

			$h/2b$	
a/b		n	0.2	0.3
1	F_I	6	1.835	1.310
		7	1.836	1.311
		8	1.836	1.311
	F_{II}	6	0.4708	0.2207
		7	0.4710	0.2209
		8	0.4710	0.2209
16	F_I	6	2.936	2.078
		7	2.940	2.081
		8	2.939	2.080
	F_{II}	6	0.9695	0.4852
		7	0.9699	0.4959
		8	0.9698	0.4958

Table 2 Comparison between the results of square and disk crack parallel to a bimaterial interface

	F_I		F_{II}	
$h/2b$	Square	Disk	Square	Disk
2.0	0.7609	0.6414	0.0008	0.0006
1.0	0.8017	0.6673	0.0096	0.0070
0.5	0.9765	0.7782	0.0699	0.052
0.4	1.093	0.8507	0.1187	0.0879
0.3	1.3146	0.9868	0.2213	0.1613
0.2	1.8503	1.2991	0.4716	0.3457

Table 1(a) shows the convergence of stress intensity factor F_I, F_{II} at (0, b) when $a/b = 1$, $a/b = 16$, $\nu_1 = \nu_2 = 0.3$, $\mu_2/\mu_1 = 0$ where the collocation point number is 20×20. It is shows that the present method gives the results with good convergence when $h/2b \geq 0.3$. The convergence becomes worse as $h/2b \to 0$ due to the large effect of interface. On the other hand, Table 1(b) indicates that 30×30 boundary collocation points have convergence to the fourth digit when $a/b = 1$ and to the third digit when $a/b = 16$.

Table 2 gives the comparison between the results of square and disk crack parallel to a bimaterial interface (Noda *et al.* 2003) for $\nu_1 = \nu_2 = 0.3$, $\mu_2/\mu_1 = 0$

4.2 Effect of Poisson's ratio

Table 3 shows the results of different Poisson's ratio when $a/b = 16$, $h/2b = 0.4$. It is shown that the results vary depending on Poisson's ratio by about 11%. The effect is not vary large even when Poisson's ratios are changed form $(\nu_1, \nu_2) = (0, 0.5)$ to $(\nu_1, \nu_2) = (0.5, 0)$. Therefore in the following calculations we simply assume $\nu_1 = \nu_2 = 0.3$.

Table 3 Dimensionless stress intensity factors F_I and F_{II} $a/b = 16$, $h/2b = 0.4$

		$\mu_2/\mu_1 = 0$	$\mu_2/\mu_1 = 0.5$	$\mu_2/\mu_1 = 2.0$	$\mu_2/\mu_1 = \infty$
F_I	$\nu_1 = 0,\ \nu_2 = 0$	1.7133	1.0918	0.9309	0.798
	$\nu_1 = 0.5,\ \nu_2 = 0.5$	1.7133	1.1378	0.8995	0.760
	$\nu_1 = 0,\ \nu_2 = 0.5$	1.7133	1.0413	0.8849	0.798
	$\nu_1 = 0.5,\ \nu_2 = 0$	1.7133	1.1688	0.9224	0.760
	$\nu_1 = 0.3,\ \nu_2 = 0.3$	1.7133	1.1135	0.9192	0.800
F_{II}	$\nu_1 = 0,\ \nu_2 = 0$	0.4035	0.1985	0.1554	–0.084
	$\nu_1 = 0.5,\ \nu_2 = 0.5$	0.4033	0.2137	0.1449	–0.082
	$\nu_1 = 0,\ \nu_2 = 0.5$	0.4035	0.1979	0.1464	–0.084
	$\nu_1 = 0.5,\ \nu_2 = 0$	0.4033	0.2204	0.1490	–0.082
	$\nu_1 = 0.3,\ \nu_2 = 0.3$	0.4034	0.2055	0.1513	–0.075

4.3 Stress intensity factor of a rectangular crack parallel to a bimaterial interface

The maximum values of F_I, F_{II} appearing at $(0, \pm b)$. Table 4 shows the maximum stress intensity factors F_I and F_{II} at $x = 0$, $y = b$ when $a/b = 1, 2, 4, 16$, $\mu_2/\mu_1 = 0, 0.1, 0.5, 2$, and $h/2b = 0.2 - \infty$. If $h/2b \le 0.5$, $\mu_2/\mu_1 \le 0.1$, the F_{II} value is lager than 10% of the F_I value, and cannot be ignored. In other cases, however, the value of F_{II} is only several percent or less of the value F_I. The values of F_{III} are smaller than F_I and F_{II}, are not given in this paper. Fig. 4 shows the distribution of the stress intensity factors F_I, F_{II} when $h/2b = 0.2$, 0.5, 2.0.

Table 4(a) Dimensionless stress intensity factors F_I and F_I^* $\nu_1 = \nu_2 = 0.3$

		F_I					F_I^*				
$h/2b$	μ_2/μ_1	0	0.1	0.5	1	2	0	0.1	0.5	1	2
0.2	$a/b = 1$	1.8503	1.2948	0.8689	0.7534	0.6786	1.3085	0.9157	0.6145	0.5328	0.4799
	$a/b = 2$	2.8567	1.6926	1.0589	0.9058	0.8082	1.6984	1.006	0.6295	0.5385	0.4805
	$a/b = 4$	2.9431	1.7903	1.1387	0.9765	0.8713	1.4715	0.8952	0.5694	0.4883	0.4357
	$a/b = 16$	2.9630	1.8123	1.1621	0.9978	0.8932	1.4010	0.8569	0.5495	0.4718	0.4223
	$(a/b = 1)/(a/b = 16)$	0.6245	0.7145	0.7477	0.7551	0.7597	0.9340	1.0686	1.1183	1.1293	1.1364
0.3	$a/b = 1$	1.3146	1.0988	0.8406	0.7534	0.6935	0.9297	0.7770	0.5945	0.5328	0.4905
	$a/b = 2$	1.9787	1.4871	1.0358	0.9058	0.8206	1.1764	0.8841	0.6158	0.5385	0.4879
	$a/b = 4$	2.0812	1.5832	1.1138	0.9765	0.8850	1.0406	0.7916	0.5569	0.4883	0.4425
	$a/b = 16$	2.0961	1.5946	1.1357	0.9978	0.9076	0.9911	0.7539	0.5370	0.4718	0.4291
	$(a/b = 1)/(a/b = 16)$	0.6271	0.6891	0.7402	0.7551	0.7641	0.9380	1.0306	1.1071	1.1293	1.1431
0.4	$a/b = 1$	1.0928	0.9827	0.8182	0.7534	0.7063	0.7728	0.6950	0.5786	0.5328	0.4995
	$a/b = 2$	1.5983	1.3357	1.0145	0.9058	0.8314	0.9502	0.7941	0.6031	0.5385	0.4943
	$a/b = 4$	1.7133	1.4373	1.0929	0.9765	0.8960	0.8567	0.7187	0.5465	0.4883	0.4480
	$a/b = 16$	1.7249	1.4449	1.1135	0.9978	0.9192	0.8156	0.6932	0.5265	0.4718	0.4346
	$(a/b = 1)/(a/b = 16)$	0.6335	0.6801	0.7348	0.7551	0.7684	0.9475	1.0026	1.0989	1.1293	1.1493

Table 4(a) Continued

		F_I					F_I^*				
$h/2b$	μ_2/μ_1	0	0.1	0.5	1	2	0	0.1	0.5	1	2
0.5	$a/b = 1$	0.9765	0.9114	0.8014	0.7534	0.7169	0.6906	0.6446	0.5668	0.5328	0.5070
	$a/b = 2$	1.3876	1.2273	0.9948	0.9058	0.8419	0.8250	0.7297	0.5914	0.5385	0.5005
	$a/b = 4$	1.5018	1.3344	1.0745	0.9765	0.9061	0.7509	0.6672	0.5373	0.4883	0.4531
	$a/b = 16$	1.5192	1.3407	1.0942	0.9978	0.9298	0.7183	0.6339	0.5173	0.4718	0.4396
	$(a/b = 1)/(a/b = 16)$	0.6428	0.6798	0.7349	0.7551	0.7710	0.9614	1.0169	1.0957	1.1293	1.1604
1.0	$a/b = 1$	0.9765	0.7899	0.7658	0.7534	0.7429	0.6906	0.5586	0.5435	0.5328	0.5254
	$a/b = 2$	1.0314	0.9992	0.9366	0.9058	0.8807	0.6131	0.5941	0.5568	0.5385	0.5236
	$a/b = 4$	1.1550	1.1079	1.0190	0.9765	0.9422	0.5775	0.5540	0.5095	0.4883	0.4711
	$a/b = 16$	1.1630	1.1205	1.0389	0.9978	0.9663	0.5499	0.5298	0.4912	0.4718	0.4569
	$(a/b = 1)/(a/b = 16)$	0.8396	0.7049	0.7371	0.7551	0.7502	1.2559	1.0544	1.1064	1.1293	1.1499
2.0	$a/b = 1$	0.7610	0.7592	0.7554	0.7534	0.7516	0.5382	0.5369	0.5342	0.5328	0.5315
	$a/b = 2$	0.8018	0.9229	0.9117	0.9058	0.9006	0.4767	0.5487	0.5420	0.5385	0.5354
	$a/b = 4$	1.0196	1.0092	0.9877	0.9765	0.9668	0.5098	0.5046	0.4939	0.4883	0.4834
	$a/b = 16$	1.0454	1.0343	1.0112	0.9978	0.9883	0.4943	0.4890	0.4781	0.4718	0.4673
	$(a/b = 1)/(a/b = 16)$	0.7280	0.7340	0.7470	0.7551	0.7605	1.0888	1.0979	1.1362	1.1293	1.1374
∞	$a/b = 1$	0.7534	0.7534	0.7534	0.7534	0.7534	0.5328	0.5328	0.5328	0.5328	0.5328
	$a/b = 2$	0.9058	0.9058	0.9058	0.9058	0.9058	0.5385	0.5385	0.5385	0.5385	0.5385
	$a/b = 4$	0.9765	0.9765	0.9765	0.9765	0.9765	0.4883	0.4883	0.4883	0.4883	0.4883
	$a/b = 16$	0.9978	0.9978	0.9978	0.9978	0.9978	0.4718	0.4718	0.4718	0.4718	0.4718
	$(a/b = 1)/(a/b = 16)$	0.7551	0.7551	0.7551	0.7551	0.7551	1.1293	1.1293	1.1293	1.1293	1.1293

Table 4(b) Dimensionless stress intensity factors F_{II} and F_{II}^* $\nu_1 = \nu_2 = 0.3$

		F_{II}					F_{II}^*				
$h/2b$	μ_2/μ_1	0	0.1	0.5	1	2	0	0.1	0.5	1	2
0.2	$a/b = 1$	0.4716	0.2202	0.0438	0	-0.0279	0.3335	0.1557	0.0310	0	-0.0197
	$a/b = 2$	0.9027	0.3420	0.0613	0	-0.0384	0.5367	0.2033	0.0364	0	-0.0228
	$a/b = 4$	0.9706	0.3713	0.0680	0	-0.0434	0.4853	0.1857	0.0340	0	-0.0217
	$a/b = 16$	0.9740	0.3767	0.0697	0	-0.0449	0.4605	0.1781	0.0329	0	-0.0212
	$(a/b = 1)/(a/b = 16)$	0.4842	0.5845	0.6284	--	0.6214	0.7242	0.8742	0.9422	--	0.9292
0.3	$a/b = 1$	0.2213	0.1336	0.0327	0	-0.0222	0.1565	0.0945	0.0231	0	-0.0157
	$a/b = 2$	0.4409	0.2347	0.0508	0	-0.0328	0.2621	0.1395	0.3020	0	-0.0195
	$a/b = 4$	0.4958	0.2631	0.0572	0	-0.0373	0.2479	0.1316	0.0286	0	-0.0187
	$a/b = 16$	0.4987	0.2657	0.0587	0	-0.0387	0.2357	0.1256	0.0278	0	-0.0183
	$(a/b = 1)/(a/b = 16)$	0.4438	0.5028	0.5571	--	0.5736	0.6640	0.7524	0.8309	--	0.8579
0.4	$a/b = 1$	0.1188	0.0796	0.0222	0	-0.0161	0.0840	0.0563	0.0157	0	-0.0114
	$a/b = 2$	0.2444	0.1509	0.0377	0	-0.0256	0.1453	0.0897	0.0224	0	-0.0152
	$a/b = 4$	0.2897	0.1772	0.0439	0	-0.0299	0.1449	0.0886	0.0219	0	-0.0178
	$a/b = 16$	0.2912	0.1787	0.0451	0	-0.0312	0.1377	0.0845	0.0213	0	-0.0147
	$(a/b = 1)/(a/b = 16)$	0.4080	0.0445	0.4922	--	0.5160	0.6100	0.6663	0.7371	--	0.7755

Table 4(b) Continued

		F_{II}					F_{II}^*				
$h/2b$	μ_2/μ_1	0	0.1	0.5	1	2	0	0.1	0.5	1	2
0.5	$a/b = 1$	0.0699	0.0493	0.0149	0	-0.0113	0.0494	0.0349	0.0105	0	-0.0080
	$a/b = 2$	0.1474	0.0982	0.0271	0	-0.0194	0.0876	0.0584	0.0161	0	-0.0115
	$a/b = 4$	0.1850	0.1215	0.0329	0	-0.0235	0.0925	0.0608	0.0165	0	-0.0118
	$a/b = 16$	0.1852	0.1228	0.0339	0	-0.0245	0.0876	0.0581	0.0160	0	-0.0116
	$(a/b = 1)/(a/b = 16)$	0.3774	0.4015	0.4395	--	0.4612	0.5639	0.6007	0.6563	--	0.6897
1.0	$a/b = 1$	0.0096	0.0073	0.0025	0	-0.0021	0.0068	0.0052	0.0018	0	-0.0015
	$a/b = 2$	0.0215	0.0160	0.0053	0	-0.0043	0.0128	0.0095	0.0032	0	-0.0026
	$a/b = 4$	0.0339	0.0250	0.0081	0	-0.0065	0.0170	0.0136	0.0041	0	-0.0033
	$a/b = 16$	0.0368	0.0272	0.0089	0	-0.0073	0.0174	0.0129	0.0042	0	-0.0035
	$(a/b = 1)/(a/b = 16)$	0.2609	0.2684	0.2809	--	0.2877	0.3908	0.4031	0.4286	--	0.4286
2.0	$a/b = 1$	0.0008	0.0006	0.0002	0	-0.0002	0.0004	0.0003	0.0001	0	-0.0001
	$a/b = 2$	0.0009	0.0007	0.0005	0	-0.0004	0.0005	0.0004	0.0003	0	-0.0002
	$a/b = 4$	0.0036	0.0027	0.0009	0	-0.0008	0.0018	0.0014	0.0005	0	-0.0004
	$a/b = 16$	0.0055	0.0042	0.0015	0	-0.0012	0.0026	0.0020	0.0007	0	-0.0006
	$(a/b = 1)/(a/b = 16)$	0.1455	0.1428	0.1333	--	0.1667	0.1538	0.1500	0.1429	--	0.1667

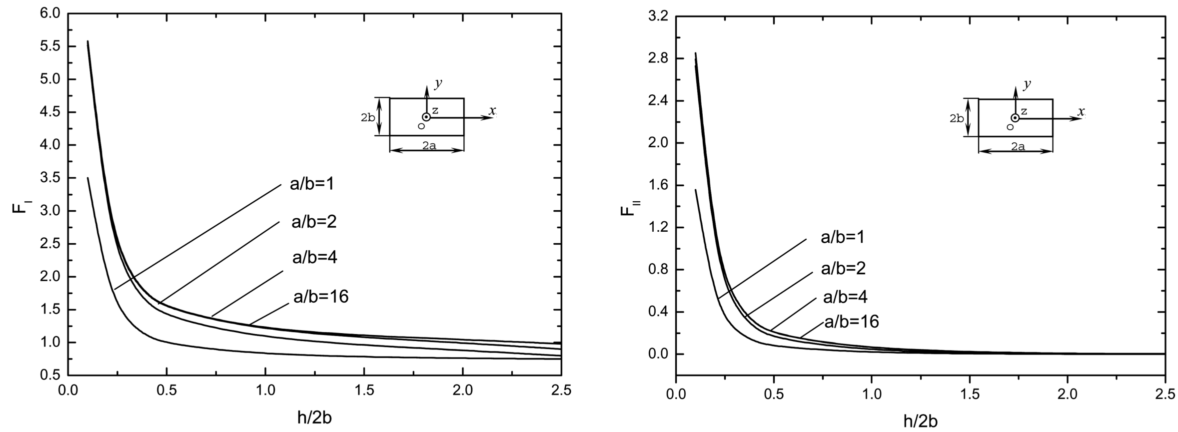

(a) F_I (b) F_{II}

Fig. 4 Variation of F_I and F_{II} when $\mu_2/\mu_1 = 0$, $\nu_1 = \nu_2 = 0.3$

In Table 4, the ratios of the results of $a/b = 1$ and $a/b = 16$ are also shown as $(a/b = 1)/(a/b = 16)$. The ratio of F_I is 0.62-0.77. On the other hand, the ratio of F_I^* is $0.93 - 1.16 \cong 1$. Fig. 4 shows F_I, F_{II} vs. $h/2b$, and Fig. 5 shows F_I^*, F_{II}^* vs. $h/2b$. It is seen F_I^* and F_{II}^* are insensitive to a/b. The $\sqrt{area}$ parameter F_I^* is found to be effective for engineering use because the effect of a/b on F_I^* is small. In the other words, different shaped cracks have almost the same values of F_I^*.

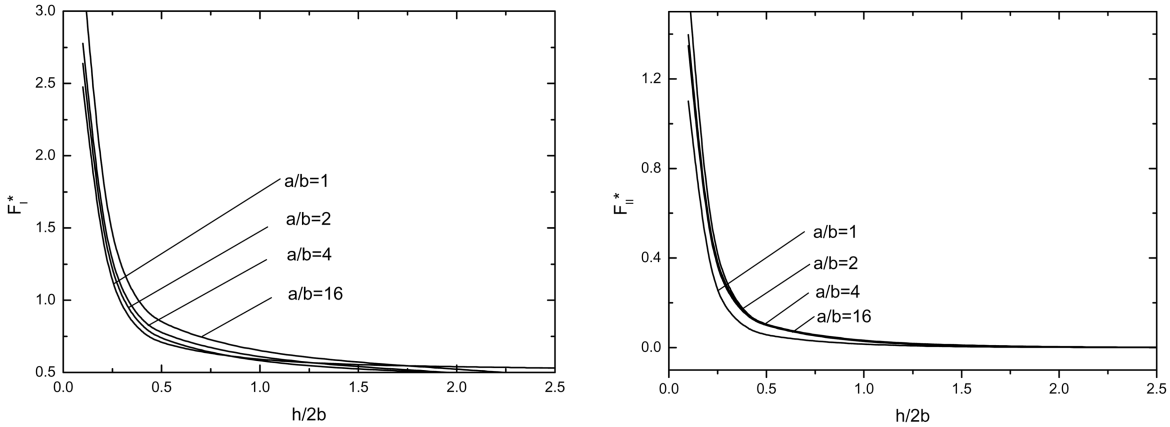

(a) F_I^* (b) F_{II}^*

Fig. 5 Variation of F_I^* and F_{II}^* when $\mu_2/\mu_1 = 0$, $\nu_1 = \nu_2 = 0.3$

6. Conclusions

In the present paper, a planar crack parallel to a bimaterials interface was considered. The stress intensity factors for a rectangular crack were calculated with varying the aspect ratio of crack, elastic constants of materials, and the distance between the crack and interface. The conclusion can be made as follows.

(1) The problem is formulated as a system of hypersingular integral equations correctly. The unknown functions of singular integral equation are approximated by using fundamental density functions and polynomials. The results show that the present method have convergence to the third digit when $a/b = 1\text{–}16$ and $h/2b \geq 0.4$ in Fig. 1. (see Table 1).

(2) The stress intensity factors are indicated in tables and figures with varying the shape of crack $a/b = 1\text{–}16$, distance form the interface $h/2b = 0.2 - \infty$, and the elastic constants $\mu_2/\mu_1 = 0 - 2.0$ when $\nu_1 = \nu_2 = 0.3$ (see Table 4). The effect of Possion's ratio is not vary large, i.e. by about 11% when $a/b = 16$, $h/2b = 0.4$.

(3) The $\sqrt{area}$ parameter F_I^* is found to be effective for engineering use because the effect of crack shape a/b on F_I^* is small. In other words, different shaped cracks have almost the same values of F_I^*.

Acknowledgements

The authors wish to thank the National Natural Science Foundation of China (No. 10872213) for the financial supports. The useful comments and suggestions provided by the reviewers are also gratefully acknowledged.

References

Afsar, A.M. and Ahmed, S.R. (2005), "Stress intensity factors for periodic edge cracks in a semi-infinite medium with distributed eigenstrain", *Struct. Eng. Mech*., **21**(1), 67-82.

Chang, J. and Xu, J.Q. (2007), "The singular stress field and stress intensity factors of a crack terminating at a bimaterial interface", *Int. J. Mech. Sci.*, **49**(7), 888-897.

Chen, M.C., Noda, N.A. and Tang, R.J. (1999), "Application of finite-part integrals to planar interfacial fracture problems in three dimensional bimaterials", *J. Appl. Mech.,* **66**, 885-890.

Chen, S.H., Wang, T.C. and Kao-Walter, S. (2003), "A crack perpendicular to the bimaterial interface in finite solid", *Int. J. Solids Struct.*, **40**(11), 2731-2755.

Cook, T.S. and Erdogan, F. (1972), "Stresses in bounded materials with a crack perpendicular to the interface", *Int. J. Eng. Sci*., **10**, 677-697.

Erdogan, F. and Aksogan, O. (1974), "Bonded half planes containing an arbitrarily oriented crack", *Int. J. Solids Struct*., **10**, 569-585.

Huang, H. and Kardomateas, G.A. (2001), "Mixed-mode stress intensity factors for cracks located at or parallel to the interface in bimaterial half planes", *Int. J. Solids Struct.*, **38**(21), 3719-3734.

Isida, M. and Nogushi, H. (1983), "An arbitrary array of cracks in bounded semi-infinity bodies under in-plane loads", *Trans. Jpn. Soc. Mech. Eng*., **49**(437), 36-45. (in Japanese)

Itou, S. (2007), "Stress intensity factors for an interface crack between an epoxy and aluminium composite plate", *Struct. Eng. Mech*., **26**(1), 99-109.

Kaddouri, K., Belhouari, M., Bouiadjra, B.B. and Serier, B. (2006), "Finite element analysis of crack perpendicular to bi-material interface: Case of couple ceramic-metal", *Comput. Mater. Sci.,* **35**(1), 53-60.

Kao-Walter, S., Stahle, P. and Chen, S.H. (2006), "A finite element analysis of a crack penetrating or deflecting into an interface in a thin laminate", Key Engineering Materials, 312, Fractures of Materials Moving Forwards, 173-178.

Kassir, M.K. and Bregman, A.M. (1972), "The stress intensity factor for a penny-shaped crack between two dissimilar materials", *J. Appl. Mech.-T. ASME*, **39**, 301-308.

Lee, J.C., Farris, T.N. and Keer, L.M. (1987), "Stress intensity factors for cracks of arbitrary shape near an interfacial boundary", *Eng. Fract. Mech*., **27**(1), 27-41.

Murakami, Y. (1985), "Analysis of stress intensity factors of mode I, II, and III inclined surface cracks of arbitrary shape", *Eng. Fract. Mech.,* **22**(1), 101-114.

Murakami, Y. and Endo, M. (1983), "Quantitative evaluation of fatigue strength of metals containing various small defects or cracks", *Eng. Fract. Mech.,* **17**(1), 1-15.

Murakami, Y. and Isida, M. (1985), "Analysis of an arbitrarily shaped surface crack and stress filed at crack front near surface", *Trans. Jpn. Soc. Mech. Eng*., **51**(464), 1050-1056. (in Japanese)

Murakami, Y. and Nemat-Nasser, S. (1983), "Growth and stability of interacting surface flaws of arbitrary shape", *Eng. Fract. Mech.*, **17**(3), 193-210.

Murakami, Y., Kodama, S. and Konuma, S. (1988), "Quantitative evaluation of effects of nonmetallic inclusions on fatigue strength of high strength steel", *Trans. Jpn. Soc. Mech. Eng*., **54**, 688-696. (in Japanese)

Noda, N.A., Ohzono, R. and Chen, M.C. (2003), "Analysis of an elliptical crack parallel to a bimaterial interface under tension", *Mech. Mater.,* **35**, 1059-1076.

Qiao, P.Z. and Wang, J.L. (2004), "Mechanics and fracture of crack tip deformable bi-material interface", *Int. J. Solids Struct.*, **41**, 7423-7444

Qin, T.Y. and Noda, N.A. (2002), "Analysis of three-dimensional crack terminating at an interface using a hypersingular integral equation method", *J. Appl. Mech*., ASME, **69**(5), 626-631.

Qin, T.Y. and Noda, N.A. (2003), "Stress intensity factors of a rectangular crack meeting a bimaterial interface", *Int. J. Solids Struct.,* **40**(10), 2473-2486.

Shibuya, T., Koizumi, T. and Iwamoto, T. (1989), "Stress analysis of the vicinity of an elliptical crack at the interface of two bonded half-spaces", *JSME Int. J.*, Series A **32**, 485-491.

Takeda, T., Shindo, Y., Narita, F. and Sanada, K. (2004), "Stress intensity factors for woven glass/epoxy laminates with cracks at cryogenic temperatures", *Mech. Adv. Mater. Struct.*, **11**(2), 109-132.

Willis, J.R. (1972), "The penny-shaped crack on an interface", *J. Mech. Appl. Math.,* **25**, 367-385.